ELSEVIER

Thermochimica Acta 396 (2003) 97–108

thermochimica acta

www.elsevier.com/locate/tca

Temperature-modulated differential scanning calorimetric measurements on pre-melting behavior of nascent ultrahigh molecular mass polyethylene

Günther W.H. Höhne*, Lada Kurelec, Sanjay Rastogi, Piet J. Lemstra

Eindhoven Polymer Laboratories, Department of Polymer Technology, The Dutch Polymer Institute, Eindhoven University of Technologie, P.O. Box 513, 5600 MB Eindhoven, The Netherlands

Received 31 December 2001; received in revised form 18 July 2002; accepted 2 October 2002

Prof. B. Wunderlich on occasion of his 70th birthday.

Abstract

Temperature-modulated differential scanning calorimetric (TMDSC) measurements on nascent ultrahigh molecular mass polyethylene (UHMMPE) in scanning as well as quasi-isothermal mode are presented. From these measurements different processes, which contribute to the modulated heat flow in the pre-melting region, both exothermic and endothermic in character, can be separated. One of them only occur on the first heating of the nascent material. Analysis of quasi-isothermal measurements, performed between 90 and 130 °C, show that there are two slow (exponential) relaxation processes with time constants of 2–5 and 10–100 min, respectively. One, exothermic in character, seems to be connected with irreversible structural changes (crystal thickening and ordering). The low activation energy (ca 40 kJ mol^{-1}) points to a chain diffusion process rather than melting and crystallization. The other process (activation energy 60 kJ mol^{-1}) seems to be endothermic. In the melting region, a slow (>100 min) 3rd relaxation process with high activation energy (300 kJ mol^{-1}) can be separated.

Keywords: TMDSC; Polyethylene; Relaxation process; Activation energy; Melting

1. Introduction

1.1. The temperature-modulated differential scanning calorimetry (TMDSC) method

Calorimetry offers the possibility to get information about processes taking place in materials if heat is exchanged with the surroundings. Conventional DSC measures the heat flow rate into a sample on heating it at a given rate:

$$\Phi(T,t) = C_p(T)\frac{\mathrm{d}T}{\mathrm{d}t} + \Phi^{\mathrm{ex.}}(T,t)x \quad (1)$$

The first term on right side characterizes the heat flow connected with the heat capacity C_p, of the sample ($\mathrm{d}T/\mathrm{d}t$ heating rate), this term is always present and greater zero. The second term, the excess heat flow rate, contains all heat flow from processes possibly occurring in the sample (melting crystallization, chemical reactions, etc.). These are usually combined with an enthalpy change of the sample and the exchange of "latent heat" with the surroundings. If there are different processes occurring in the same moment,

* Corresponding author.
E-mail address: g.w.h.hoehne@tue.nl (G.W.H. Höhne).

0040-6031/02/$ – see front matter
PII: S0040-6031(02)00528-2

the common DSC measures only the net heat flow rate of the processes.

The separation of the latent heat of a process from the total signal is normally straight forward: as the heat capacity C_p does not change very much with temperature its contribution to the heat flow rate can normally be approximated by a straight line (the baseline) which can easily be subtracted from the measured signal yielding the excess heat flow rate and (after integration) the latent heat of the process. The situation is more complicated, if different processes contribute to $\Phi^{\text{ex.}}$, e.g. if exothermic and endothermic processes (e.g. crystallization and melting) occur at the same time. In such cases, only the net excess heat flow rate is measured, this could be about zero. Although such processes occur in the sample, this is not visible in the measured curve.

The method of TMDSC offers in certain cases the possibility to separate time-dependent processes (having a non-zero complex excess heat capacity) from normal (static) heat capacity and the apparent heat capacity connected with latent heat from processes which are not time-dependent, or very fast, compared to the time scale of modulation.

The mathematical background for a proper TMDSC evaluation is shortly as follows: we start from a sinusoidal modulation, i.e. the temperature change reads:

$$T(t) = T_1 + \beta_0 t + T_\text{A} \sin(\omega t) \tag{2}$$

with β_0 the underlying heating rate, T_A the amplitude and $\omega = 2\pi f$ the angular frequency of modulation. The derivative of the temperature is the heating rate:

$$\frac{\mathrm{d}T}{\mathrm{d}t} = \beta_0 + T_\text{A}\omega\cos(\omega t) \tag{3}$$

introducing this into Eq. (1) yields:

$$\Phi(T,t) = C_p(T)\beta_0 + C_p(T)T_A\omega\cos(\omega t) + \Phi^{\text{ex.}}(T,t) \tag{4}$$

The excess heat flow rate can be expanded in a Taylor series around T_u:

$$\Phi^{\text{ex.}}(T,t) = \sum_{s=0}^{\infty} \frac{1}{n!} \frac{\partial^s \Phi^{\text{ex.}}(T_\text{u},t)}{\partial T^s} (T - T_\text{u})^s \tag{5}$$

defining T_u the "underlying" temperature change $T_\text{u}(t) = T_1 + \beta_0 t$, the excess heat flow can be described with Eq. (2). For small temperature amplitudes T_A, we get a rather good approximation:

$$\Phi^{\text{ex.}}(T,t) \approx \Phi^{\text{ex.}}(T_\text{u},t) + \frac{\partial \Phi^{\text{ex.}}(T_\text{u},t)}{\partial T} T_\text{A}\sin(\omega t) \tag{6}$$

Introducing this into Eq. (4) yields:

$$\Phi(T,t) = C_p(T)\beta_0 + \Phi^{\text{ex.}}(T_\text{u},t) + C_p(T)T_\text{A}\omega\cos(\omega t) + \frac{\partial \Phi^{\text{ex.}}(T_\text{u},t)}{\partial T} T_\text{A}\sin(\omega t) \tag{7}$$

This can be separated into a non-periodic "underlying" and a periodic part. Obviously the heat capacity as well as the excess heat flow basically contributes to both parts of the signal. From Eq. (7) we get the "underlying" part

$$\Phi_\text{u}(T,t) = C_p(T_\text{u})\beta_0 + \Phi^{\text{ex.}}(T_\text{u},t) \tag{8}$$

and the periodic part

$$\tilde{\Phi}(T,t) = C_p(T)T_\text{A}\omega\cos(\omega t) + \frac{\partial \Phi^{\text{ex.}}(T_\text{u},t)}{\partial T} T_\text{A}\sin(\omega t) \tag{9}$$

During reactions with a non-zero excess heat, there is always an in-phase as well as out-of-phase part present in the modulated signal (formally resulting in a complex apparent heat capacity!) but the contribution from $\Phi^{\text{ex.}}$ may be small if the temperature derivative of the excess heat flow rate at the temperature T_u is small compared to the product ωC_p.

Eq. (9) has the form $A\cos(x) + B\sin(x)$, where A is always positive and B positive or negative depending on the excess heat flow rate being endo- or exothermic in character. The amplitude of the sum is, however, always larger than A and the resulting signal is shifted in phase, but in a different direction for positive (endothermic) and negative (exothermic) contributions from the excess heat flow rate (see Fig. 1).

On the other hand, the periodic (modulated) part of the measured heat flow rate can be written as

$$\tilde{\Phi}(T,t) = \Phi_\text{A}\cos(\omega t + \delta) \quad \text{with}$$
$$\Phi_\text{A} = \sqrt{(C_p(T)T_\text{A}\omega)^2 + \left(T_\text{A}\frac{\partial \Phi^{\text{ex.}}}{\partial T}(T_\text{u},t)\right)^2} \quad \text{and}$$
$$\delta = \arctan\frac{(\partial \Phi^{\text{ex.}}/\partial T)(T_\text{u},t)}{C_p(T)\omega} \tag{10}$$

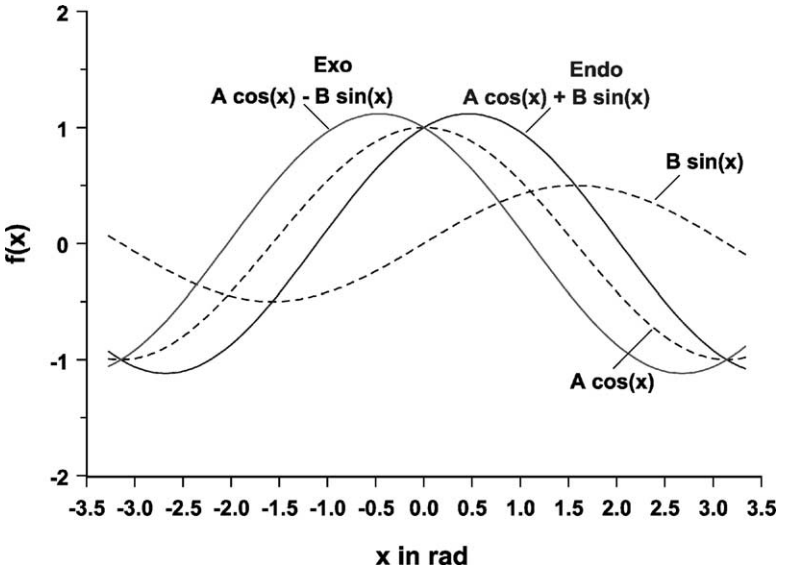

Fig. 1. Illustration of Eq. (9), both the sum and the difference of both RS terms causes an increase of the amplitude but with a different phase shift.

In other words, the amplitude of the periodic heat flow rate increases always if an excess heat flow rate is present, whereas the underlying signal increases for positive (endothermic) but decreases for negative (exothermic) $\Phi^{\text{ex.}}$ events (see Eq. (7)). This, in the first moment unexpected fact should be born in mind when discussing the reversing signal in the presence of processes contributing latent heat. The only way to decide whether the latent heat is endo- or exothermic in character is to look at the phase angle which turns out to be an absolutely essential quantity in this context.

Often the amplitude Φ_{A} of the modulated part of the heat flow rate is used to calculate the (apparent) specific heat capacity of the sample (the reversing heat capacity):

$$C_p = \frac{\Phi_{\text{A}}}{m\omega T_{\text{A}}} \tag{11}$$

Because of the slow heat conduction, of course, a frequency-dependent calibration factor has to be included to get proper values. In the case that excess heat flow rates from latent heat are involved, we get from Eq. (11) with Eq. (10)

$$C_p^{\text{apparent}} = \sqrt{(C_p(T))^2 + \left(\frac{1}{m\omega}\frac{\partial \Phi^{\text{ex.}}}{\partial T}(T_{\text{u}}, t)\right)^2} \tag{12}$$

where $C_p(T)$ the classical (static) specific heat capacity. From Eq. (12) follows, that the measured apparent heat capacity is *not a simple sum* of the static heat capacity and an excess heat capacity (from the latent heat contribution), but the magnitude (absolute value) of the sum of two rectangular vectors. Formally the apparent specific heat capacity can be described as the magnitude of a complex quantity C_p^*

$$C_p^{\text{apparent}} = |C_p^*| = \sqrt{(C_p')^2 + (C_p'')^2} \tag{13}$$

with $C_p(T)$ as the real part and the excess heat capacity from the excess heat flow rate as the imaginary part. It should be emphasized that the time dependency of the excess heat flow producing processes has been neglected so far, i.e. these processes are considered to react on temperature changes much faster than one period of modulation. If, however, the time scale of such a process is comparable with the period of modulation, the above derived relations become much more complicated and Eq. (9) and consequently Eq. (12) then contains additional time/frequency-dependent terms, but these terms only reduce the magnitude particularly at higher frequencies. The absence of time dependence of the excess heat flow results in the largest amplitude of the modulated, reversing, signal

and thus in the largest apparent heat capacity. Every time dependence leads to a complex heat capacity, where both real and imaginary part are frequency-dependent. This has been shown in many papers in literature (e.g. by Schawe, Merzlyakov, Toda and others) and shall not be repeated here.

1.2. Application of TMDSC on ultrahigh molecular mass polyethylene (UHMMPE)

The aim of this paper is to demonstrate the power of the TMDSC method for investigations and separation of different processes, time-dependent or not, with a non-zero excess (complex) heat capacity in the light of a special polymer example.

From polymers it is known, that on heating endothermic pre-melting as well as exothermic crystallization and re-ordering takes place at temperatures well below the visible melting region (peak). Consequently polymers seem to be very interesting materials to be investigated with TMDSC. This has been done for different polymers and numerous papers exist on this topic (see the review article of Wunderlich [1]). In particular PE is a material with very high chain mobility already well below the melting region. A special PE, nascent UHMMPE, is recently in the center of interest. This material is synthesized with catalysts in solution at rather low temperatures (well below the crystallization temperature). The synthesis conditions cause immediately crystallization of the chain coming from the active center of the catalyst. The outcome are conglomerates of poorly ordered crystals of very long chains with a rather low number of entanglements and a low number of inter-crystal molecules. This reactor powder offers some very interesting possibilities to get a polyethylene material with high quality mechanical properties [2]. The chain mobility seems to be high in nascent UHMMPE this makes crystal growth and perfection possible on annealing well below the melting point. To get more insight into the nature of this process we performed TMDSC experiments with nascent UHMMPE.

2. Experimental

Different types of nascent UHMMPEs have been investigated. In this paper, we confine ourselves to present the results from a special nascent UHMMPE (M_w ca 4 Mg mol^{-1}, M_w/M_n 5.7) from DSM (The Netherlands) synthesized with a Ziegler–Natta catalyst at temperatures well below the dissolution temperature. The reactor powder was investigated as received, from common DSC runs a crystallinity of 65% was determined, TEM images showed disordered micro-lamellar conglomerates with crystallite sizes of about 10 mm × 30 nm. Samples of 0.7–3.5 mg mass were weighted with a precision balance and encapsulated in standard (crimped) Al-pans of well known (and always the same) mass. Almost identical empty pans were used in the reference side and for the baseline run. Nitrogen was used as purge gas at a rate of 25 ml min^{-1}.

We used a standard Perkin-Elmer DSC-7 (calibrated as usual) which we modified (with a commercial precision function generator) to enable a sinusoidal temperature modulation.

The TMDSC measurements were usually done with an underlying heating rate β_0 of 0.1 or 0.5 K/min, which was proved to be low enough to ensure no influence on the modulated part of the signal. Different frequencies f in the range between 2 and 125 mHz (with $\omega = 2\pi f$) were used to prove the frequency influence on the results. The temperature amplitude T_A was selected low enough to ensure linear response, and in such a way, that the heating rate dT/dt was always greater zero and the same for the different frequencies (i.e. heating only mode; ωT_A = const.). This was done to exclude possible influences of different heating rates on the processes in the sample and the measurements. From the sample run results, the empty pan run results (taking the same measuring parameters and phase position) were subtracted before further evaluation, in order to reduce surroundings and/or apparatus influences on the measured curve.

The measured (modulated) heat flow rate signal $\Phi(T, t)$ was first treated as usual [3]. By "gliding integration" over one period we got the "underlying" part $\Phi_u(t)$ which was subtracted from the measured signal to get the periodic part $\tilde{\Phi}(T, t)$. From the latter the calculation of the apparent heat capacity (magnitude and phase shift) was done with a Windows^{TM} program using the mathematical procedure described in Ref. [4]. The proper (frequency-dependent) calibration factor for the heat capacity magnitude (needed to correct for errors caused by heat transfer influences

[5,6]) was determined by comparing the calculated heat capacity in the liquid state of PE at 150 °C with the respective value from literature [7].

3. Results and discussion

In Fig. 2, the magnitude (modulus, absolute value) and phase shift of the apparent (complex) heat capacity of nascent UHMMPE is plotted together with the C_p-curve calculated from the underlying heat flow (which equals the conventional DSC curve). As a remarkable result, the magnitude curve is clearly larger than the underlying curve in the pre-melting temperature region. There is an excess heat capacity in that region which is much larger in the modulated (reversing) part of the heat flow signal than in the underlying curve.

To get more information about the process causing such behavior, we compared the magnitude curve from the first heating run with those of the respective cooling and second heating runs (Fig. 3). In the temperature region between 90 and 120 °C, the first heating of the nascent material gives the largest apparent heat capacity. This drops distinctly in the following cooling from the melt and the second heating run, at least in the temperature region before the melting peak comes up, which, however, is shifted to much lower temperatures than in the first run. The smallest excess heat capacity is found for the C_p-curve calculated from the conventional DSC run (which is almost like the underlying C_p-curve). To get an impression where the static (thermodynamic) heat capacity of PE is, the literature values for the amorphous and crystalline phase of PE [7] are included too.

To see whether the apparent heat capacity is time-dependent, we investigated the behavior at different frequencies. The results are shown in Fig. 4: with increasing frequency the apparent heat capacity in the pre-melting region drops to the value of the underlying curve. Careful analysis shows that the respective process is time-dependent: if the frequency is too large, it cannot follow the temperature changes from the modulation anymore and the excess heat capacity of the process drops to zero. (Remark: the proper frequency-dependent calibration factor has again been determined by fitting the measured apparent heat capacity in the liquid state above the melting peak to the literature values in this region.)

For further evaluation, we have to separate the different excess heat capacities from the static (vibrational) heat capacity of the sample. The “excess heat capacity”, connected with processes taking place in the sample, is in literature often defined as the dif-

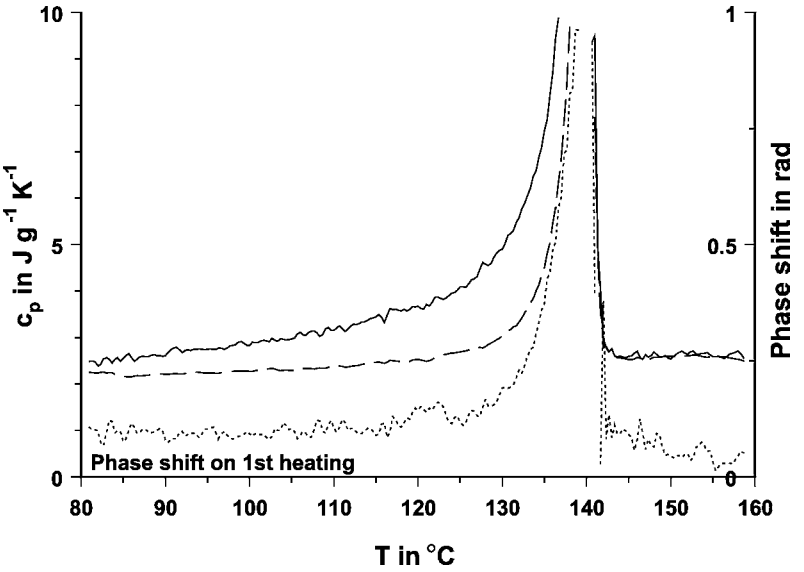

Fig. 2. TMDSC curves of nascent UHMMPE (mass: 1.6 mg, heating rate: 0.5 K/min, frequency: 12.5 mHz, period: 80 s, T_A: 53 mK). Solid line: magnitude of reversing apparent C_p, dotted line: phase shift, dashed line: underlying apparent C_p.

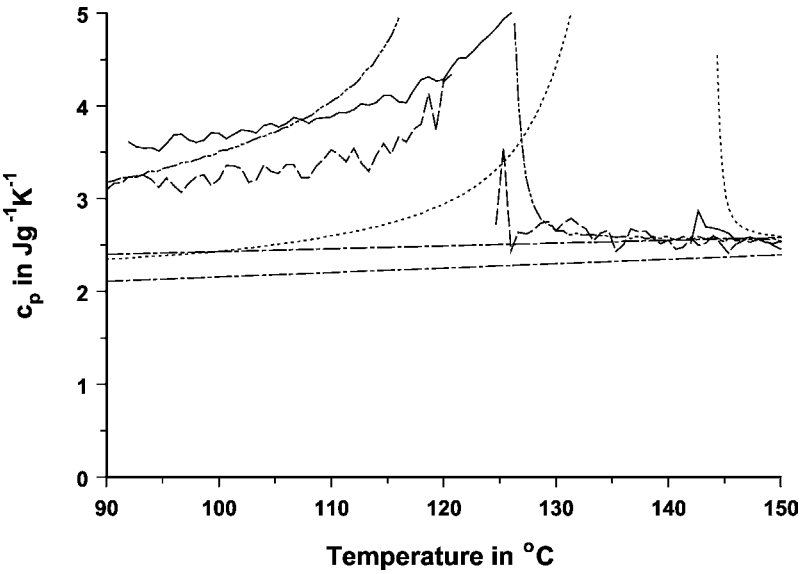

Fig. 3. Apparent C_p TMDSC curves of nascent UHMMPE on 1st heating (solid) subsequent cooling(dashed) and 2nd heating (dash-dot-dotted) together with the conventional DSC curve at 10 K/min (dotted) and literature values of static C_p (crystal and amorphous phase, dash-dotted [7]) (mass: 0.7 mg, heating rate: 1.0 K/min, frequency: 12.5 mHz, period: 80 s, T_A: 106 mK).

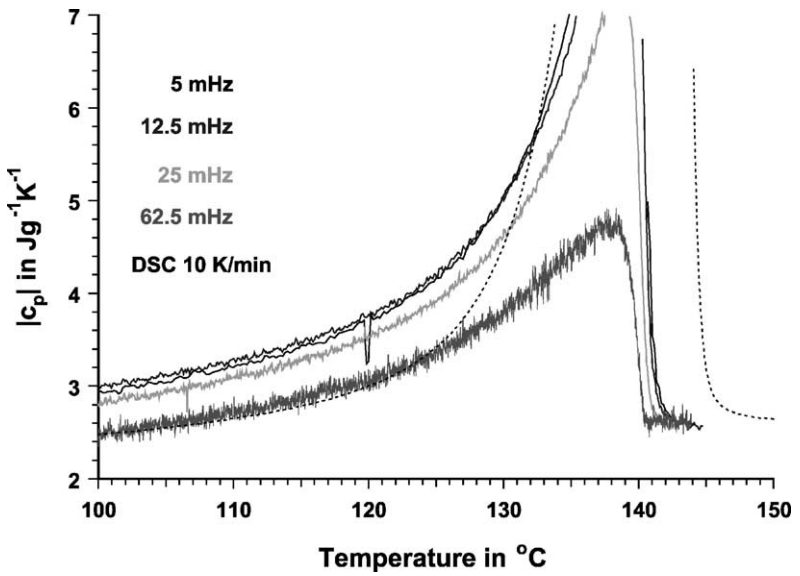

Fig. 4. TMDSC apparent curves of nascent UHMMPE on 1st heating at different frequencies together with the conventional DSC curve at 10 K/min (dotted) (mass: ca 4 mg, heating rate: 0.1 K/min, $\omega T_A = 3.6$ mK rad s^{-1}).

ference between the real static heat capacity of the semi-crystalline sample, calculated with the known degree of crystallinity, and the measured C_p from the reversing, modulated, part of the signal. But, as Eq. (12) shows, such an "excess heat capacity" is *not* the right one if there is an excess heat flow from the processes in question. In such a case the true excess heat capacity must be calculated by means of Eqs. (12) or (13):

$$C_p^{\text{ex.}} = |C_p''| = \sqrt{(C_p^{\text{apparent}})^2 - (C_p(T))^2} \tag{14}$$

where $C_p(T)$ the static specific heat capacity of the sample, this is the baseline of the melting peak, which unfortunately cannot be determined without further assumptions, as it may contain more than the vibrational components of the heat capacity. Because of these difficulties we have, in a first step, determined the simple but wrong "excess heat capacity" (from the difference) as well. The result of this evaluation, published elsewhere [8], is nevertheless helpful regarding the understanding and interpretation of the different pre-melting processes in nascent UHMMPE.

Combination of the methods and comparison of conventional and TMDSC curves makes it possible to separate different excess processes, if we remind the theoretical considerations presented in Section 1. With this background, comparing all the curves in Figs. 2–4 with one another, we have to draw the following conclusions:

- There are at least three processes taking place in the sample in the pre-melting region.
- One process is irreversible and only visible in the reversing signal of the 1st run of the nascent material.
- One process is reversible and unchanged visible in the reversing signal of the second and further runs.
- There must be one more process which is *not* visible in the reversing signal, but needed to cause an almost zero net heat flow in the pre-melting region of the underlying curve of the first run.
- At least one of these processes must be exothermic and one endothermic to give the measured low value of the net heat flow rate in the underlying (conventional) DSC curve of the first run.
- One processes contributing to that part of the reversing signals which go beyond the conventional DSC signal is time-dependent and the time constant is within the reciprocal frequency window of our measurements.

What processes can that be? Androsch and Wunderlich [9] recently suggested six different processes which could distribute to the apparent heat capacity in the melting region of polymers:

1. The vibrational heat capacity, the largest contribution, always reversible and endothermic in character.
2. The emergence of dynamically changing conformational isomers (e.g. trans to gauche conformation changes), reversible and endothermic as well.
3. Reversible melting, reversible even for small temperature changes and endothermic.
4. Crystal perfection and thickening on annealing, rather slow irreversible and weak exothermic process in partial crystalline non-equilibrium state.
5. "Secondary crystallization", partial reversible and exothermic in character.
6. Initial, "primary" crystallization, the biggest latent heat process, strictly irreversible and exothermic.

For nascent UHMMPE we have to select the processes from this list in such a way that the experimental findings are satisfied and, in particular, the net heat flow rate is low, as the underlying curve tells us.

To learn something about the endo- or exothermic character, we have to look at the phase angle in the temperature region in question. As the measurement of the *absolute* phase in TMDSC is still a problem, we have to look at the *relative* phase shift. In Fig. 5, the respective curves of the 1st and 2nd run are plotted together. To be able to compare the curves properly we have shifted the temperature scales relative to the peak maximum temperature. The decrease of the apparent heat capacity is obvious as well as a distinct difference in the phase signal in the pre-melting region. During the 1st run, the phase shift is significant lower than in the 2nd run. From this follows, taking the relations of Fig. 1 into account, that the irreversible process of the 1st run must be exothermic in character. Whereas the remaining part of the apparent excess heat capacity belongs to an endothermic process because of the remaining positive phase shift in the 2nd run. It should, however, be emphasized that such an evaluation of the phase signal is only possible very qualitatively. Nevertheless, the found

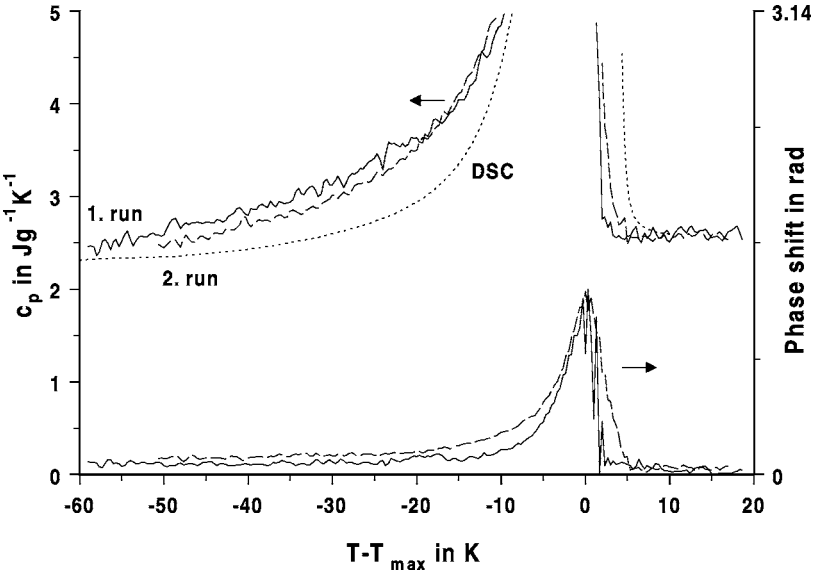

Fig. 5. TMDSC apparent C_p and phase angle curves of nascent UHMMPE (mass: 1.5 mg, heating rate: 0.5 K/min, frequency: 12.5 mHz, period: 80 s, T_A: 53 mK). 1st run (solid) and 2nd run (dashed) shifted in temperature relative to the melting peak—together with the conventional DSC 1st run (dotted).

differences in-phase angle are significantly supporting the exothermic character of the process in question.

Falling back on the list of possible processes, we would like to interpret our experimental findings as follows. The irreversible, exothermic process visible only in the 1st run of nascent UHMMPE is the (4) process (crystal perfection), the reversible endothermic process could be the reversible melting process, which has been reported before for other PEs (see e.g. Ref. [10]). To get the proper balance of the net heat flow rate in the conventional DSC curve there must be another exothermic process, not visible in the modulated signal, compensating the melting heat of the second process. This could be the (6) process of the above list, the primary crystallization which does not appear in the reversing signal as the temperature derivative $\partial\phi^{\text{cryst.}}/\partial T$ is very small normally.

Performing quasi-isothermal TMDSC measurements with nascent UHMMPE at different temperatures below the melting peak, we investigated the change of the apparent heat capacity in time as well (Fig. 6, dotted curves). Obviously there is an irreversible (time-dependent) as well as a constant component present and all curves are well above the vibrational heat capacity of the material (compare Fig. 3) and even above the underlying curve at the temperature in question. Here the question arises, what is the proper $C_p(T)$ value to be used for the calculation of the excess heat capacity via Eq. (14). We really do not know, so we first tried to deconvolute the *measured* (*apparent*) heat capacity signal and found a sum of two exponential decays plus a time-independent signal [8]. If we, however, assume that the reversing signal—which we got in a second run after annealing the sample at 120 °C—yield the proper $C_p(T)$ value at that temperature, we can calculate a better approximation of the excess heat capacity of the time-dependent component. The resulting curves are included in Fig. 6 as well.

For further evaluation, we have to make an assumption concerning the processes involved. The simplest possible time-dependent and temperature activated process is an enthalpy relaxation process:

$$H(T,t) = H_0(T)\,\mathrm{e}^{-t/\tau(T)} \quad \text{with} \quad \tau = \tau_0\,\mathrm{e}^{E_A/RT} \tag{15}$$

where τ the relaxation time, E_A the activation energy. Such a process is connected with a heat flow

$$\frac{\mathrm{d}H}{\mathrm{d}t} = \Phi^{\text{ex.}}(T,t) = -\frac{H_0(T)}{\tau(T)}\mathrm{e}^{-t/\tau(T)} \tag{16}$$

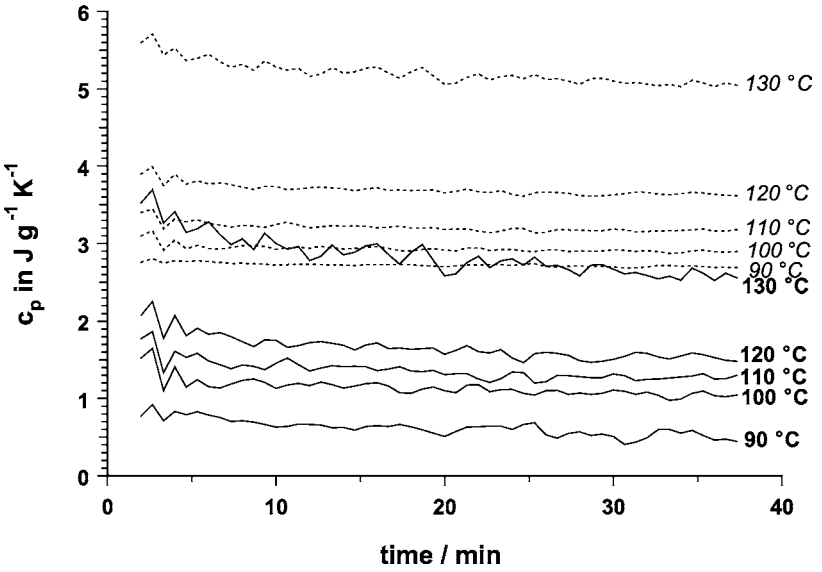

Fig. 6. Excess heat capacity (solid) calculated with Eq. (14) from the measured apparent heat capacity (dotted); quasi-isothermal TMDSC measurements at different temperatures (mass: 2–3 mg, frequency: 12.5 mHz, period: 80 s, T_A: 53 mK).

From this, the amplitude of the modulated excess heat flow rate can be calculated via Eq. (10). The result is somewhat complex, but the time dependence (at a given temperature) is, however, again a simple exponential one. The same is true for the excess heat capacity signal, which is calculated via Eq. (11). (Remark: the *apparent* heat capacity is, of course, *not* a simple sum of an exponential and a constant function (see Eq. (12)), but has a rather complex time dependence.)

Starting from the named assumptions, we tried to further analyze the excess heat capacity signals plotted in Fig. 6 and found that they can be described with a sum of two exponential functions (see Table 1), whereas a fit with a single exponential does not lead to satisfactory results. To get more insight into the character of the processes, the phase signals (see Fig. 7) have been analyzed too. From Eq. (10), with the assumption of Eq. (16), follows, that tan δ should relax exponentially as well. Looking at Fig. 7, we indeed see the relaxation of the phase angle as expected. We can furthermore see that in the temperature region 90–110 °C, the phase increasingly relaxes toward more positive values. Then at 120 °C this relaxation process becomes smaller again and the phase seems to decrease somewhat at times above 20 min. At 130 °C, the phase shift changes the sign, now it decreases in time. The exponential fit results are collected in Table 2.

Table 1
Result of fitting $a_1 e^{-t/\tau_1} + a_2 e^{-t/\tau_2} + a_0$ to the quasi-isothermal excess heat capacity results of nascent UHMMPE

T (°C)	a_1 (J g^{-1} K^{-1})	t_1 (min)	a_2 (J g^{-1} K^{-1})	t_2 (min)	a_0 (J g^{-1} K^{-1})
90	0.5	4.6	0.5	>50	0.3
100	0.7	2.5	0.5	>50	0.7
110	0.8	1.9	0.4	25	1.2
120	0.9	1.5	0.5	16	1.5
130	1.0	2.7	1.4	67	1.8
136	3.0	5	1.3	225	7.7
139	20	3.4	1.1	140	3.7

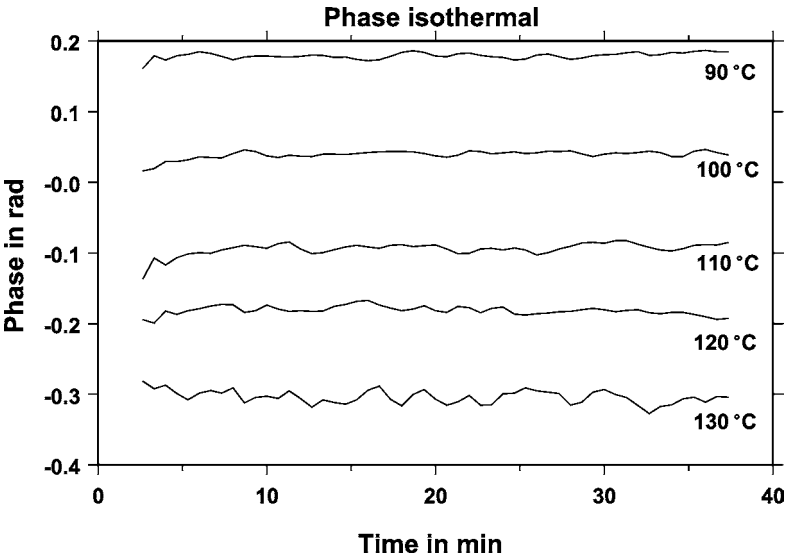

Fig. 7. Measured phase angle (shifted arbitrarily) from the quasi-isothermal measurements of Fig. 6.

In Fig. 8, the additional results of two more isothermal measurements in the melting region are shown.

What do we learn from these findings? There are obviously different processes, one, which is predominant below 130 °C and exothermal in character, as the direction of the phase shift tells us, and another one, starting above 120 °C, which is endothermic. In the melting region above 130 °C, a third one is coming in. All processes are superimposed in the apparent heat capacity together with the static heat capacity, but they seem also to be present in the excess heat capacity, which we got via Eq. (14), and in the phase signal.

The results are, of course, very uncertain, there are a lot of assumptions and the signals are weak and noisy, so careful measurements should be done to prove these results, before we can draw conclusions from the polymer science point of view. The objective of this paper is, however, to show the power and possibilities of careful TMDSC measurements to get more insight into time and temperature-dependent processes in polymers.

Table 2
Result of fitting $a_1\,e^{-t/\tau_1} + a_2\,e^{-t/\tau_2} + a_0$ to the quasi-isothermal tan d results of nascent UHMMPE

T (°C)	a_1 (rad)	t_1 (min)	a_2 (rad)	t_2 (min)	a_0 (rad)
90	−0.14	>50	–	–	−0.001
100	−0.075	2.5	–	–	−0.009
110	−0.17	1.9	–	–	−0.021
120	−0.2	8	+0.2	11	−0.03
130	+0.06	2.7	–	–	+0.02
136	+0.2	5.4	+0.2	220	−0.01
139	+1.4	5.6	+0.2	65	−0.05

However, as a result the excess C_p decreases (exponentially) in time and the time constant depend on temperature. Assuming the processes to be of Arrhenius type (see Eq. (15)), we can determine the activation energies from the slopes in a $\ln \tau$ via $1/T$ plot (see Fig. 9) and get 40 ± 10, 60 ± 10 and 300 ± 50 kJ mol^{-1}, respectively, for the three processes. The first two numbers are of the same order of magnitude as the activation energy of the α-process determined from mechanical measurements [11]. The activation energy of the third process occurring in the melting region is, however, much higher, it is more like that of the β-process (glass transition) or that of the viscosity of the liquid.

How to interpret the findings? From the polymer physical point we would restrict ourselves to some preliminary remarks, a more detailed discussion will be published elsewhere [12]. There must be (at least) two different processes, one endothermic and one exothermic, occurring together in the sample in the pre-melting region so that we get an almost zero net heat flow rate (see the underlying signal).

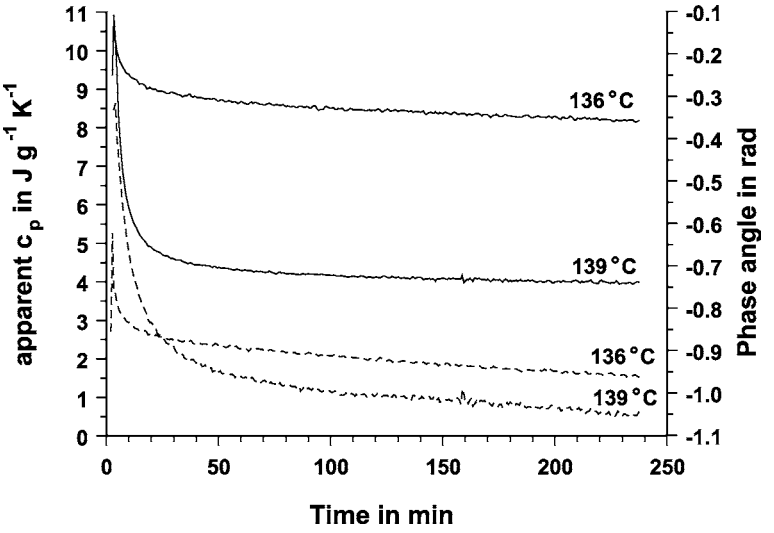

Fig. 8. Apparent heat capacity (solid) and phase angle (dashed) from quasi-isothermal TMDSC measurements in the melting region of nascent UHMMPE (mass: 2–3 mg, frequency: 12.5 mHz, period: 80 s, T_A: 53 mK).

The first exothermic process, visible in the excess heat capacity and phase signal at lower temperatures, could be the ordering and perfection of the crystals. This process is compensated by an endothermic process which does *not* contribute to the modulated *excess* heat capacity, it could be an additional (abnormal) part of the static heat capacity (e.g. by conformational changes) or an endothermic process not visible at all in the modulated but only in the underlying signal.

At temperatures above 120 °C another, from the phase shift endothermic, process becomes visible in the modulated signal. This endothermic process is

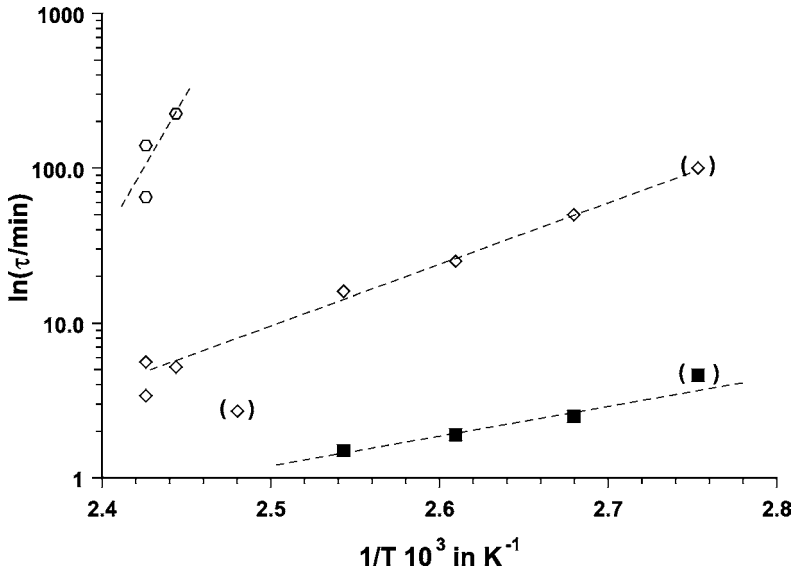

Fig. 9. Activation diagram of all the processes listed in Tables 1 and 2, the slope gives the activation energy (solid symbols: exothermic, open symbol: endothermic).

visible in the phase angle as well as in the excess heat capacity signal, it could be something like reversible melting. As the lower underlying curve tells us, even that process is almost compensated by another exothermic process, which is *not* visible in the modulated signal. The latter could be some irreversible crystallization, which normally is not seen in the apparent or excess heat capacity part since the temperature derivative of that process is very weak.

In the melting region, a third rather slow process with large temperature dependence and high activation energy comes in. This again endothermic process seems to be something like dissolution or "superheating" of the crystallites in the surrounding already liquid phase, since it is related to the mobility of larger parts of the molecule as is the case for viscosity properties.

From the six possible processes, which Androsch and Wunderlich [9] suggest as contributing to the apparent heat capacity, we would choose processes 1–4 to explain our findings, whereas the crystallization (process 5 and 6) contributes to the underlying heat flow only. The processes taking place at lower temperatures have an activation energy of 40–50 kJ mol^{-1}, this equals the enthalpy of fusion of ca 10 CH_2 units, a value much to low for a chain to be separated from the crystal. A careful analysis of the frequency behavior of the irreversible excess heat capacity of the first run yield a "corner frequency" (maximum of the imaginary part, where the amplitude drops to about 50% of the low frequency value) of that process $f_0 = 0.024$ Hz at 110 °C [8]. This value fits very well to the mechanical α-process of PE [11,13] and even the activation energy of that process is in the same order of magnitude. Obviously the chain diffusion through the crystals plays a role in the pre-melting region.

4. Conclusions

TMDSC is a suitable method to study pre-melting processes in polymers. By comparing and evaluating the underlying as well as the apparent and excess heat capacity and the phase shift of scanning as well as quasi-isothermal TMDSC experiments, it is possible to separate the different processes involved. The phase signal established as essential to determine the endo- or exothermic character of the processes, which both lead to an increase of the magnitude of the apparent heat capacity. Because of the vectorial addition of the exothermic excess and endothermic heat capacity contributions, we get always a positive excess heat capacity, whereas the net heat flow, as measured in conventional DSC, remains almost zero in this temperature region. As a consequence, there is only a small change of the degree of crystallinity detectable, much smaller than the time-integral over the excess heat capacity necessitates. The excess heat capacity connected to this irreversible process is lower than the total excess heat capacity on heating. The remaining part of the excess heat capacity, which even exist in modulated cooling runs, may be related to processes like reversible melting (or melting crystallization) and even to conformational changes.

References

[1] B. Wunderlich, Prog. Polym. Sci. 391 (2002) 51.
[2] S. Rastogi, L. Kurelec, P.J. Lemstra, Macromolecules 31 (1998) 5022.
[3] B. Wunderlich, Y. Jin, A. Boller, Thermochim. Acta 238 (1994) 277.
[4] G.W.H. Höhne, Thermochim. Acta 304/305 (1997) 209.
[5] G.W.H. Höhne, Thermochim. Acta 330 (1999) 93.
[6] G.W.H. Höhne, M. Merzlyakov, C. Schick, Thermochim. Acta, in press.
[7] B. Wunderlich, et al., Athas databank, 2000. http://web.utk.edu/~athas.
[8] G.W.H. Höhne, L. Kurelec, Thermochim. Acta 377 (2001) 141.
[9] R. Androsch, B. Wunderlich, Macromolecules 33 (2000) 9076.
[10] R. Androsch, B. Wunderlich, Macromolecules 32 (1999) 7238.
[11] P.U. Mayr, Dissertation, Universität Ulm, 1998.
[12] G.W.H. Höhne, L. Kurelec, S. Rastogi, in preparation.
[13] A. Müller, W. Pechhold, W.v. Soden, Proceedings of Deutscher Verband für Materialprüfung e.V., Aachen, 1975, p. 148.